Quantifying Constructability Performance of 3D Concrete Printing via Rheology-Based Analytical Models

Jacques Kruger(✉), Stephan Zeranka, and Gideon van Zijl

Division for Structural Engineering and Civil Engineering Informatics, Stellenbosch University, Stellenbosch, South Africa
pjkruger@sun.ac.za

Abstract. 3D printing of concrete (3DPC) is a developing automation technology that can promote further industrialisation in the construction industry. 3DPC has complex rheological requirements, namely low material viscosity for ease of pumping but high viscosity for constructability. Greater emphasis is therefore placed on the rheology of cement-based composites used for 3DPC compared to conventional construction techniques. Thixotropic materials demonstrate the material performance required for 3DPC. This research presents the work of Kruger et al., who developed a bi-linear thixotropy model [1] specifically for 3DPC materials. This model demonstrates the degree of thixotropy of a material and the static yield shear stress evolution after it has been extruded. A buildability model [2] predicts the maximum number of filament/printing layers achievable, which is based on the bi-linear thixotropy model. Lastly, a rheology-based filament shape retention model [3] determines the maximum height of a filament layer where no plastic yielding at a material point will occur. The three aforementioned models are applied in this research in order to quantify the constructability of 3DPC by only conducting rheology tests and no mechanical tests. A circular hollow column is 3D printed that validates the models presented in this research. The buildability model predicted 52 filament layers whereas 54 layers were obtained experimentally before failure, yielding a conservative 3DPC construction height prediction of 3.7%.

Keywords: 3D concrete printing · Rheology · Buildability · Shape retention · Modelling

1 Introduction

3D printing of concrete (3DPC) entails the pumping and extrusion of concrete in its plastic state. Printable concrete requires a balance between pumpability at low viscosity (to avoid high pump pressures) and buildability at high viscosity, while retaining the homogeneity of the concrete during the pumping and extrusion phase. A feasible range in printable concrete viscosity therefore exists, as depicted in Fig. 1. Due to the conflicting requirements of pumpability and buildability of 3DPC, different approaches have been developed to characterise 3DPC, most notably based on rheological or mechanical properties in the fresh state (green strength).

V. Mechtcherine et al. (Eds.): RheoCon 2019/SCC 2019, RILEM Bookseries 23, pp. 400–408, 2020.
https://doi.org/10.1007/978-3-030-22566-7_46

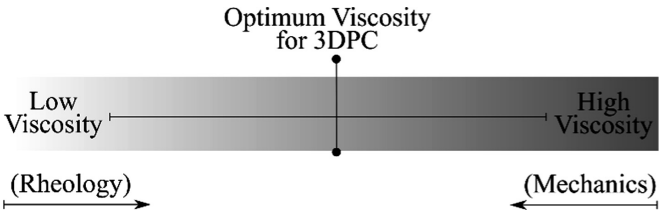

Fig. 1. Viscosity range of a 3D printable concrete indicating rheological characterisation preferred for low viscosities and mechanical characterisation for high viscosities.

State of the art literature on 3DPC modelling is mainly based on the mechanical characterisation of materials. Suiker [4] proposed a mechanistic buildability model for 3DPC that requires a material's green strength properties as input parameters. Similarly, Wolfs et al. [5] developed a numerical model for 3DPC based on green strength properties. However, this research builds on current 3DPC literature that is based on rheological characterisation [6].

Kruger et al. [1] developed a bi-linear thixotropy model specifically for 3DPC. Thixotropic material behaviour is deemed the most appropriate for 3DPC as a distinct difference exists between the static and dynamic yield shear stress. Thus, the material's viscosity decreases while being agitated during the pumping process and then increases after the agitation is removed. The model defines the re-flocculation rate (R_{thix}) that is a measure of the degree of thixotropy of a material. Buildability [2] and filament shape retention [3] models are incorporated that are also based on rheological characterisation.

This research applies these models in practice in order to demonstrate the relative ease with which the constructability process of 3DPC can be quantified by only characterising the rheology of a material. This is achieved by performing a rheological characterisation of the standard 3DPC material at Stellenbosch University (SU) and thereafter 3D printing a circular hollow column to validate the models.

2 Analytical Models

2.1 Bi-linear Thixotropy Model

A novel bi-linear thixotropy model for 3DPC is developed by Kruger et al. [1]. This model builds on the thixotropy model that is proposed by Roussel [7] by accounting for both re-flocculation (R_{thix}) and structuration (A_{thix}) mechanisms, as indicated in Fig. 2. R_{thix} is mainly a physical process resulting from interparticle forces, specifically interatomic and intermolecular forces on a particle's surface, and typically reaches equilibrium in a few hundred seconds. A_{thix} is mainly a chemical process that is influenced by the early formation of hydration products, consequently yielding a decrease in concrete plasticity. The study by Kruger et al. [1] found that R_{thix} is a better indicator of thixotropic behaviour suitable for 3DPC than A_{thix}.

The practical aspect of the model is that it portrays a material's static yield shear stress evolution after it has been extruded from the nozzle as a function of resting time. Thus, the shear history is accounted for, which is then immediately followed by re-flocculation and thereafter structuration. The shear history incorporates the shearing action induced by the pump and hose during the 3DPC process. Due to this shearing action, a material's microstructure is broken down from the static to dynamic yield shear stress that is denoted by $\tau_{D,i}$ in Fig. 2. After cessation of the agitation i.e. when the material exits the nozzle, Brownian motion will result in re-flocculation of the particles consequently rebuilding the material's original microstructure before shear was induced, denoted as $\tau_{S,i}$ which is the material's initial static yield shear stress. Thereafter the material structurates until the hydration process comes into full effect. A material's shear strength can be obtained as a function of resting time with the following equations:

$$\tau_S(t) = \tau_{D,i} + R_{thix} \cdot t \quad for \quad [t \leq t_{rf}] \tag{1}$$

$$t_{rf} = \frac{\tau_{S,i} - \tau_{D,i}}{R_{thix}} \tag{2}$$

$$\tau_S(t) = \tau_{S,i} + A_{thix} \cdot (t - t_{rf}) \quad for \quad [t > t_{rf}] \tag{3}$$

Where $\tau_S(t)$ is the static yield shear stress of the material at time (t) after deposition and t_{rf} the time period over which re-flocculation occurs as illustrated in Fig. 2.

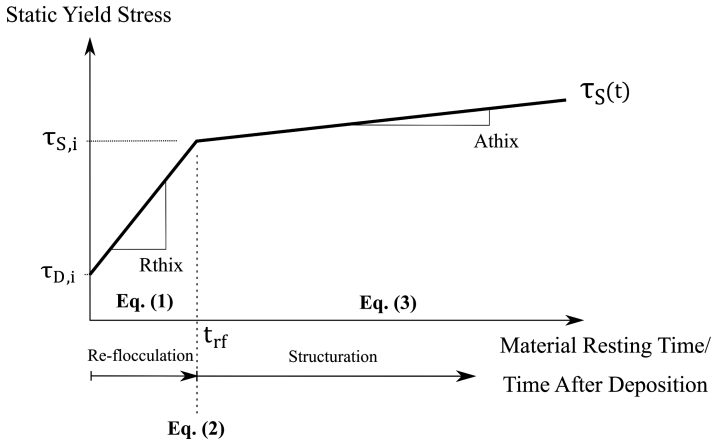

Fig. 2. Bi-linear thixotropy model that depicts the static yield shear stress evolution as a function of material resting time after deposition.

2.2 Buildability Model

An analytical model is developed by Kruger et al. [2] that quantifies the buildability performance of a material for 3DPC, in particular the maximum number of layers

achievable before failure occurs. This model only accounts for physical nonlinearity i.e. plastic yielding of the bottom critical filament layer and not geometrical nonlinearity such as elastic buckling. The resistance provided by the material against plastic yielding, namely the static yield shear stress, is incorporated via Eqs. 1 to 3. Thus, the buildability model is primarily based on rheology and not on green strength. An a priori check is performed to determine which one of the final two Eqs. 5 or 6, is to be employed:

$$\textit{If} \qquad \frac{d}{dt}\left(\frac{\rho \cdot g \cdot h_l \cdot v \cdot 10^{-3}}{2 \cdot l_p \cdot F_{AR}} \cdot t\right) \geq \frac{\tau_{S,i} \cdot R_{thix}}{\tau_{S,i} - \tau_{D,i}} \tag{4}$$

$$\textit{Then use} \qquad N_L = -\left[\frac{\tau_{D,i}}{\left(\frac{R_{thix} \cdot l_p}{v}\right) - \left(\frac{\rho \cdot g \cdot h_l}{2.10^3 \cdot F_{AR}}\right)}\right] \tag{5}$$

$$\textit{Else use} \quad N_L = -\left[\frac{\tau_{S,i} + \left(\frac{A_{thix} \cdot \left(\tau_{D,i} - \tau_{S,i}\right)}{R_{thix}}\right)}{\left(\frac{A_{thix} \cdot l_p}{v}\right) - \left(\frac{\rho \cdot g \cdot h_l}{2.10^3 \cdot F_{AR}}\right)}\right] \tag{6}$$

Where ρ is the material density (kg/m^3), g the gravitational constant (m/s^2), h_l the filament layer height (mm), v the printing speed (mm/s), l_p the print path length per layer (mm), N_L the number of filament layers and F_{AR} the strength correction factor based on the aspect ratio of the filament layer.

Concrete in its plastic state demonstrates similar behaviour to cohesive soils, i.e. both possess less capacity in tension than in compression. In this case, failure in compression is due to relative movement of particles resulting in shear failure and not by crushing of constituents. This pressure-dependent shear failure is best defined by the Mohr-Coulomb failure criterion. However, more material parameters are required to employ this failure criterion, such as cohesion (c) and interparticle friction (φ). Both are functions of time that will consequently require more laborious data acquisition. Therefore, a simplified approach is adopted that focuses on the principle stress state within a filament layer. As depicted in Fig. 3a, the aspect ratio of a filament layer will determine the stress state, in particular a uniaxial or triaxial stress state, provided that sufficient friction is present to prevent slip. The area wherein a triaxial stress state is present is referred to as being confined. For an aspect ratio of 2, failure typically occurs in the middle of the specimen due to uniaxial stress conditions that yield maximum shear stress. This is evident in unconfined uniaxial compression tests (UUCT) whereby failure is depicted by the Tresca criterion, or maximum shear stress theory, and also forms the lower bound of the Mohr-Coulomb failure criterion. Confinement increases as the aspect ratio of a filament layer decreases, consequently yielding higher apparent compressive strengths relative to the strength at an aspect ratio of 2 [8], as depicted in Fig. 3b. This is synonymous to reaching the upper bound of the Mohr-Coulomb failure criterion, known as the Rankine or maximum normal stress theory. The model is

simplified by incorporating strength correction factors (F_{AR}) that are normalised to unity at an aspect ratio of 2, as depicted in Fig. 3b.

In essence, the vertical building rate obtained from print-specific parameters is equated to the strength development curve depicted in Fig. 2. This yields Eqs. 5 and 6, however, the vertical building rate that is expressed in terms of normal stress is converted to the equivalently induced shear stress by means of the Mohr-Coulomb failure criterion. In order to negate additional material tests, the lower bound Tresca failure criterion is adopted. Confinement within filament layers, which has a significant influence on the total bearing capacity, is accounted for by means of strength correction factors for various filament layer aspect ratios. More detailed information is presented in [2].

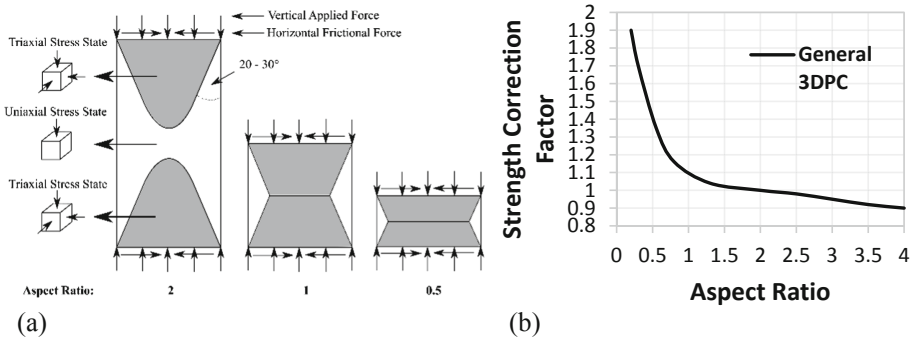

Fig. 3. (a) Confinement within filament layers of different aspect ratios and (b) strength correction factors (F_{AR}) for various filament aspect ratios.

2.3 Shape Retention Model

Kruger et al. [3] developed a quasi-static analytical model to determine the maximum filament layer height whereby plastic yielding at any material point will not occur under self-weight, thus preventing significant deformation after extrusion. Filament shape retention is not only a prerequisite for good buildability performance, but also for adequate surface aesthetics of 3DPC elements. The model is based on the dynamic yield shear stress ($\tau_{D,i}$). Therefore, material shear history is of crucial importance to obtain accurate predictions.

A cross-section segment of a filament layer is illustrated in Fig. 4. Plane strain behaviour is assumed due to the continuous lateral support provided in the longitudinal direction of the filament layer. As for the buildability model, it is assumed that sufficient friction is present to induce confinement in the bottom part of the filament layer, as depicted in Fig. 4a. Consequently, a horizontal stress termed σ_2 is induced. The plane strain conditions specify that $\sigma_3 = \upsilon \cdot (\sigma_1 + \sigma_2)$, where υ is the material's Poisson's ratio. The vertically induced stress due to self-weight is $\sigma_1 = \rho \cdot g \cdot h_l$. By assessing the maximum and minimum stress combinations on a Mohr circle, the following shape retention expressions are presented for failure zones 1, 2 and 3 in Fig. 4b respectively:

$$H_{max} = \frac{2 \cdot \tau_{D,i}}{\rho \cdot g} \tag{7}$$

$$H_{max} = \frac{2 \cdot \tau_{D,i} \cdot (1 - \upsilon)}{\rho \cdot g} \tag{8}$$

$$H_{max} = \frac{2 \cdot \tau_{D,i}}{(1 - \upsilon) \cdot \rho \cdot g} \tag{9}$$

Where H_{max} is the maximum filament layer height at which plastic deformations will not occur. By interpreting Eqs. 7 to 9 parametrically, it can be seen that Eq. 8 will always govern. More detailed information is presented in [3].

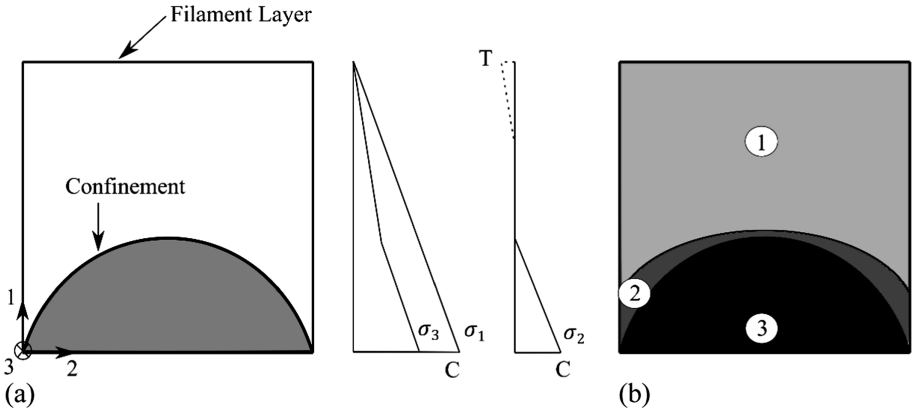

Fig. 4. (a) Cross-section of a filament layer with confinement in the bottom and corresponding principle stresses indicated to the right, and (b) three failure zones within a filament layer.

3 Experimental Procedure

The standard 3DPC mix at SU, given in Table 1, is employed in this research. Initially a 20L batch is prepared for the rheological characterisation via the Germann ICAR rheometer. A stress growth test is performed at various material resting time intervals. This test involves the application of a constant shear rate and the shear stress measured as a function of time. The shear induced via the pump process is approximately replicated with the rheometer by correlating the rheometer's vane speed to that of the pump's screw. The shear induced via the hose is taken into account by correlating the rheometer shear duration to the time it takes material to exit the nozzle. A shear rate of $1s^{-1}$ is obtained based on a rotational speed of 0.2 rev/s. The shear duration is equal to 60 s based on a hose length of 3.5 m and a print speed of 60 mm/s. This is a simplified approach to yield roughly the same induced shear by the rheometer as during the printing process. This shear rate and duration is used for all rheological measurements. A stress growth test is performed at the following resting intervals (s): 0, 10, 20, 30, 40, 50, 60,

90, 120, 180, 1200, 2400 and 3600. A single-batch approach is followed; however, it is acknowledged that segregation may occur on the vane's perimeter at higher concrete ages. R_{thix} and A_{thix} are then calculated and the static yield shear stress evolution curve plotted. More details regarding the test procedure can be obtained in [1].

The buildability (Eqs. 4–6) and shape retention (Eqs. 7–9) models are applied after the rheological characterisation and data processing have been executed. A circular hollow column with diameter 250 mm is 3D printed until failure occurs. A 25 mm diameter circular nozzle is used at a deposition height of 10 mm to yield a layer width and height of 30 mm and 10 mm respectively. The concrete density, obtained by filling a known volume (1 L) and measuring the sample's mass, is 2150 kg/m^3. The Poisson's ratio is assumed to be 0.3, following the work and assumptions made by Wolfs et al. [5] and Suiker [4]. Based on the aforementioned data, l_p is calculated as 785 mm and F_{AR} as 1.7 from Fig. 3b.

4 Results and Discussions

The static yield shear stress evolution curve as well as the thixotropy parameters are indicated in Fig. 5. The material has a re-flocculation rate of 6.88 Pa/s, which is more than 6 times that of its structuration rate of 1.08 Pa/s. The material is regarded as highly thixotropic. The buildability model (Eq. 6) predicted that 52 filament layers would be obtained. The governing expression of the shape retention model (Eq. 8) predicted a maximum stable filament layer height of 76 mm.

The 3D print is illustrated in Fig. 6. 54 filament layers are obtained in 12 min at a layer height of 10 mm; thus, a total height of 540 mm is obtained. Plastic yielding of the bottom filament layers instigated global failure of the printed element. No filament layer deformation is observed, except for a slight undulating pattern on the printed element's surface due to irregular pump frequencies.

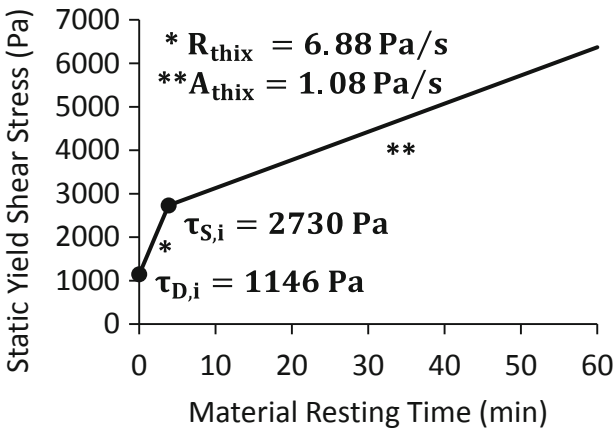

Fig. 5. Static yield shear stress evolution curve depicting the initial static and dynamic yield shear stresses as well as the re-flocculation and structuration rates.

Table 1. Standard SU 3DPC mix constituent quantities.

Constituent	kg
Cement	579
Fly ash	165
Silica fume	83
Fine aggregate	1167
Water	261
Superplasticizer	1.48%, by binder mass

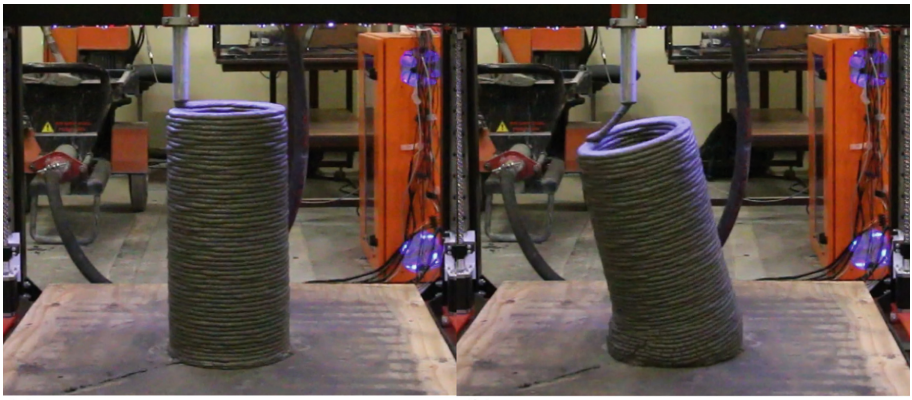

Fig. 6. (a) 3D printed circular hollow column just before failure occurs and (b) plastic yielding of bottom filament layers results in global failure of the printed column.

The models presented by Kruger et al. [1–3] are thus validated. The buildability model in particular predicted a conservative building height of 3.7% lower than the actual, stable 3D printed column height. This is the most accurate prediction by the model to date, as previously an underprediction of 8.3% was achieved [2].

5 Conclusion

The models developed by Kruger et al. for thixotropy, buildability and shape retention of 3DPC elements are presented in this research. These models are practically applied in order to demonstrate their ease of use by only characterising a material's rheology. After the print-specific and material parameters were determined, the models predicted a maximum of 52 filament layers before failure occurs as well as a maximum stable filament layer height of 76 mm. Failure of the 3D printed 250 mm diameter circular hollow column occurred after the deposition of 54 layers at a layer height of 10 mm. A good surface finish was obtained due to insignificant filament deformation after extrusion. The buildability model predicted a building height of 3.7% lower than the actual, stable 3D printed column height.

Acknowledgement. The authors gratefully acknowledge Mr Seung Cho's assistance with the experimental work. This research is funded by The Concrete Institute (TCI) and the Department of Trade and Industry of South Africa under THRIP Research Grant TP14062772324.

References

1. Kruger PJ, Zeranka S, van Zijl GPAG (2019) An ab initio approach for thixotropic characterisation of (nanoparticle-infused) 3D printable concrete. Constr Build Mater 224:372–386

2. Kruger PJ, Zeranka S, van Zijl GPAG (2019) 3D concrete printing: a lower bound analytical model for buildability performance quantification. Autom. Constr. 106:10294
3. Kruger PJ, Zeranka S, van Zijl GPAG (2019) A rheology-based quasi-static shape retention model for digitally fabricated concrete
4. Suiker ASJ (2018) Mechanical performance of wall structures in 3D printing processes: theory, design tools and experiments. Int J Mech Sci 137:145–170. https://doi.org/10.1016/j.ijmecsci.2018.01.010
5. Wolfs RJM, Bos FP, Salet TAM (2018) Early age mechanical behaviour of 3D printed concrete: Numerical modelling and experimental testing. Cem Concr Res 106:103–116. https://doi.org/10.1016/j.cemconres.2018.02.001
6. Roussel N (2018) Rheological requirements for printable concretes. Cem Concr Res 112:76–85. https://doi.org/10.1016/j.cemconres.2018.04.005
7. Roussel N (2006) A thixotropy model for fresh fluid concretes: Theory, validation and applications. Cem Concr Res 36:1797–1806. https://doi.org/10.1016/j.cemconres.2006.05.025
8. Lamond JF, Pielert JH (2006) Significance of tests and properties of concrete and concrete-making materials. ASTM International, West Conshohocken ISSN 9780803155206